RESEARCH ARTICLE

Spatial variability in chromophoric dissolved organic matter for an artificial coastal lake (Shiwha) and the upstream catchments at two different seasons

Diep Dinh Phong · Yeonjung Lee · Kyung-Hoon Shin · Jin Hur

Abstract Selected water quality parameters and spectroscopic characteristics of dissolved organic matter (DOM) were examined during two different seasons for an artificial coastal lake (Shiwha Lake in South Korea), which are affected by seawater exchange due to the operation of a tidal power plant and external organic loadings from the upstream catchments. The coastal lake exhibited much lower concentrations of organic matter and nutrients than the upstream sources. The spectroscopic properties of the lake DOM were easily distinguished from those of the catchment sources as revealed by a lower absorption coefficient, lower degree of humification, and higher spectral slopes. The observed DOM properties suggest that the lake DOM may be dominated by smaller molecular size and less condensed structures. For the lake and the upper streams, higher absorption coefficients and fluorescence peak intensities but lower spectral slopes and humification index were found for the premonsoon versus the monsoon season. However, such seasonal differences were less pronounced for the industrial channels in the upper catchments. Three distinctive fluorophore groups including microbial humic-like, tryptophan-like, and terrestrial humic-like fluorescence were decomposed from the fluorescence excitation-emission matrix (EEM) of the DOM samples by parallel factor analysis (PARAFAC) modeling. The microbial humic-like component was the most abundant for the industrial channels, suggesting that the component may be associated with anthropogenic organic pollution. The terrestrial humic-like component was predominant for the upper streams, and its relative abundance was higher for the rainy season. Our principal component analysis (PCA) results demonstrated that exchange of seawater and seasonally variable input of allochthonous DOM plays important roles in determining the characteristics of DOM in the lake.

Introduction

Dissolved organic matter (DOM) is a heterogeneous mixture consisting of carbohydrates, proteins, lignins, organic acids, and various uncharacterized structures such as humic substances (HS) (Thurman 1985). DOM is considered to be an important element for aquatic ecosystems owing to its multiple functionalities, including nutrient sources, light attenuation, changing metal toxicity, and microbial respiration (Mulholland 2003). DOM is introduced into aquatic systems through external (allochthonous) and internal (autochthonous) sources.

From the standpoint of DOM cycling, a coastal environment can be categorized into a transition zone where both external and internal sources are mixed together and various biogeochemical transformation processes occur. Several factors associated with upstream catchments such as hydrology, geomorphology, land use/land cover, soil types, and seasonality are likely to govern the quantity and the quality of the DOM that is exported into the coastal environments (Stedmon et al. 2003; Kowalczuk et al. 2009; Yamashita et al. 2011). In nearby oceanic water, meanwhile, other processes such as microbial degradation, photo-oxidation, and algal productivity were proposed as critical factors to determine the temporal

Responsible editor: Céline Guéguen

D. D. Phong · J. Hur (✉)
Department of Environment and Energy, Sejong University,
Seoul 143-747, South Korea
e-mail: jinhur@sejong.edu

Y. Lee · K.-H. Shin
Department of Environmental Marine Sciences, Hanyang University,
Keongki-do, Ansan 426-791, South Korea

and spatial variations in DOM (Romera-Castillo et al. 2011; Guo et al. 2011; Maie et al. 2012).

The Shiwha Lake, an artificial coastal lake, is located on the west coast of South Korea adjacent to the industrial cities of Ansan and Siheung. This lake is surrounded by a 12.6-km-long dike (constructed in 1994) as part of the development of 173 km^2 of a tidal flat. This estuary originally provided good habitats for aquatic organisms, receiving water discharge from the upstream watershed through streams and runoff (KICOX 2011). However, the dike construction has led to a serious deterioration of water quality in the region due to the insufficient circulation of the enclosed lake water and the continuous input of anthropogenic pollutants from nearby industrial complexes (KORDI 1999). The average chemical oxygen demand (COD) in the midregion of the lake before the construction of the dike was 4 mg L^{-1}, but it increased up to 15 mg L^{-1} after the completion of the construction. To cope with the problem, the South Korean government designated Lake Shihwa as a special management zone, and it opened a water gate in a middle of the dike in 2001 to allow water exchange with the adjacent sea (Ra et al. 2011). In 2011, a tidal power plant equipped with its power capacity of 254 MW was constructed to promote seawater circulation and to supply electric power to the nearby industrial complex (Cho et al. 2012). In spite of the recent effort, however, continuous pollution input from the upstream industrial complexes and the urban areas has been a concern for maintenance of a sustainable ecosystem for this area (Yoo et al. 2009; Moon et al. 2012).

Excitation-emission matrix (EEM) fluorescence spectroscopy has been widely utilized as the simplest and most effective method for probing the composition and the sources of DOM in aquatic environments. Stedmon et al. (2003) used parallel factor analysis (PARAFAC) to successfully decompose a large data set of EEMs into several separate components representing its unique fluorescence features. Many subsequent studies proved that combining EEM with PARAFAC provided more reliable and plentiful information on the fluorescence signals of DOM in various aquatic ecosystems (Murphy et al. 2008; Yamashita et al. 2010; Yamashita et al. 2008; Guo et al. 2011). There were many reports that successfully explored the spatial and temporal variability of DOM in coastal regions using EEM-PARAFAC analyses (Yamashita et al. 2011; Chari et al. 2012).

A few studies have been reported on ecological and environmental evaluations of the Shiwha Lake since the construction of the tidal power plant, in which the accumulation of heavy metals in sediments and bioaccumulation of benthic organisms were highlighted (Ra et al. 2011; Won et al. 2012). To date, however, there has been no investigation on DOM in the coastal region affected by the operation of a tidal power plant. It is thus required to examine the temporal and spatial variability of DOM in the lake, tracking its sources. Therefore,

this study aimed at (1) exploring the distributions of DOM and its spectroscopic characteristics within Lake Shiwha and the upper streams at two different seasons (i.e., the monsoon and the premonsoon seasons) and (2) tracking the sources of the lake DOM by employing various spectroscopic techniques including EEM-PARAFAC and multivariate statistical analysis.

Materials and methods

Study area and sample collection

The Shiwha Lake is located on the west coast of South Korea (between 126° 31′–127° 00′ E and 37° 11′–37° 23′ N, Fig. 1). The depth reaches 17.9 m in the middle zone with the average value of 4.5 m, and the area is approximately 79.4 km^2. The total watershed area is 476.5 km^2 and the lengths of the inflowing streams are approximately 10 km. The water-holding capacity of the lake reaches up to 323,769,000 m^3 (Cho et al. 2012). Approximately 13,000 mills involving mechanical (48 %), electrical/electronic (19 %), petrochemical (8.3 %), steel (5.7 %), and textile companies (3.5 %) are currently operated in the upstream industrial complex areas. The total population of the two cities of Shiheung and Ansan exceeds 1 million (KICOX 2011). The average rainfall in this region for the year 2012 was 1,719 mm. Intense rainfalls occur mainly in the monsoon season from June to September. The amount of rainfall during this period of 2012 accounts for 82.4 % of the total annual rainfall (www.wamis.go.kr).

A total of 15 sampling sites were selected to fully reflect the spatial variability of the water quality and DOM of the lake and the surrounding areas (Fig. 1). Sampling was conducted twice in 2012 during two separate nonrain events of the premonsoon (May 14–15) and the monsoon seasons (September 5–7). For each sampling season, eight samplings were made from the surface and the bottom layers at four different lake sites (L1–L4). Five samples (I1–I5) were collected from the channels receiving treated wastewater and surface runoff from the industrial complexes. Four samples (U1–U4) were collected from the upper streams surrounded by forested and agricultural areas. Two sampling sites (E1 and E2) represented an estuary region, which connects the upper streams with the lake. The collected samples (4 L) were refrigerated and stored in an ice box, moved to a laboratory, and kept in a refrigerator. All sample analyses were carried out within a week after their collection except for biochemical oxygen demand (BOD), which was completed within 12 h.

General water quality and DOM spectroscopic measurements

Measured general water quality parameters included BOD, COD, total nitrogen (TN), total dissolved phosphorus (TDP),
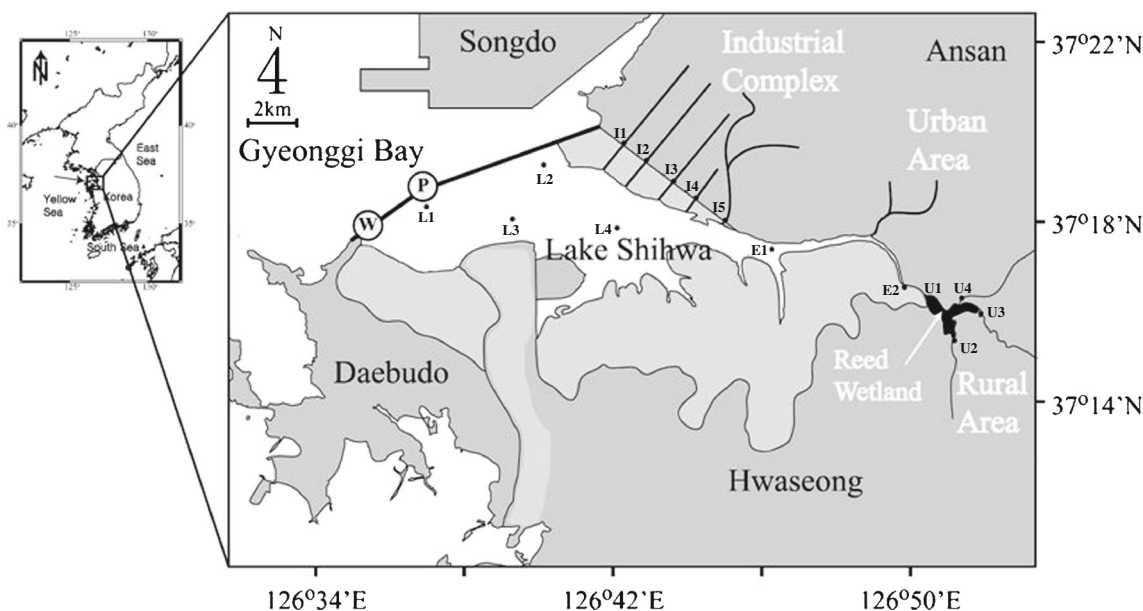
Fig. 1 Study area and the sampling locations

and chlorophyll *a* (Chl *a*). All the measurements were made based on standard protocols (APHA 2005).

An aliquot (100 ml) of each collected sample was filtered using a prewashed 0.45-μm membrane filter (cellulose acetate, Advantec) for DOM analyses. Dissolved organic carbon (DOC) concentrations (mg C L^{-1}) were determined using a Shimadzu V-CPH analyzer. Ultraviolet (UV)–visible spectra from 250 to 600 nm were recorded using a UV–visible spectrophotometer (Evolution 60, Thermo Scientific) with a 1-cm quartz cuvette. Specific UV absorbance (SUVA) values of the samples were calculated by multiplying DOC concentration-normalized UV absorbance at 254 nm by a factor of 100 (i.e., $100 \times UV_{254} / DOC$) (Weishaar et al. 2003). The spectral slopes of $S_{275–290}$ and $S_{350–400}$ were obtained by the ratios of the two best fit regression lines from the natural log-transformed absorption spectra of the filtered samples at the wavelength ranges between 275 and 295 nm and between 350 and 400 nm, respectively (Helms et al. 2008). In addition, an absorption coefficient at 375 nm (a375) was measured for chromophoric DOM (CDOM) concentrations.

Fluorescence EEMs were measured with a luminescence spectrometer (LS-55, PerkinElmer) by scanning the emission spectra from 280 to 550 nm at 0.5-nm increments and stepping through excitation wavelengths from 250 to 500 nm at 5-nm increments. Excitation and emission slits were adjusted to 10 and 5 nm, respectively, and the scanning speed was set at 1,200 nm min^{-1}. To limit second-order Rayleigh scattering, a 290-nm cutoff filter was used for all the measurements. When the UV absorbance of the samples at 254 nm exceeded 0.05 cm^{-1}, the corresponding samples were appropriately diluted to avoid the inner filter correction (Hur et al. 2007). The background fluorescence EEM from a blank solution

(Milli-Q water) was also taken into account. Fluorescence intensity was normalized in quinine sulfate equivalent (QSE) units, where 1 QSU corresponded to the maximum fluorescence intensity for 1 μg L^{-1} of quinine in 0.1 N H_2SO_4 at the excitation/emission of 350/450 nm (Coble et al. 1998). The fluorescence index (FI) was calculated as the ratio of the emission intensities at 450 to 500 nm for an excitation wavelength of 370 nm (McKnight et al. 2001). FI values have been used to differentiate between allochthonous and autochthonous DOM sources. Humification index (HIX) was calculated according to a definition suggested by Zsolnay et al. (1999) with an exception of using the excitation wavelength of 255 nm instead of 254 nm. Higher HIX values are typically associated with the characteristics of soil-derived DOM such as a higher content of aromaticity, a lower rate of mineralization, and a lower percentage of oxygen-containing functional groups (Fuentes et al. 2006).

PARAFAC modeling

For this study, PARAFAC modeling was performed using MATLAB 7.0 (MathWorks, Natick, MA, USA) with the DOMFluor Toolbox (http://www.models.life.ku.dk). The details of the modeling are well described elsewhere (Stedmon et al. 2003; Kowalczuk et al. 2009; Nguyen et al. 2013). The split-half analysis was used to validate the identified components and the number.

Statistical analyses

Statistical analyses including correlation coefficients and PCA were performed using XLSTAT (Addinsoft, New York, NY,

USA). Differences in parameters were evaluated using the p values based on Student's t test. The relationships among variables were evaluated using regression and correlation analyses. Shapiro-Wilk test was performed to confirm the normality of the measured parameters.

Results and discussion

Spatial and seasonal variations of general water quality parameters

The collected samples exhibited large variations in the organic matter concentrations ranging from 0.7 to 5.9 mg L^{-1} for BOD, from 5.2 to 72.6 mg L^{-1} for COD, and from 1.8 to 23.9 mg L^{-1} for DOC, respectively (Table 1). The small portion of BOD to COD indicates that the organic matters are mostly constituted by nonbiodegradable fractions. The nutrient concentrations varied from 0.5 to 4.7 mg L^{-1} and from 0.023 to 0.177 mg L^{-1} for TN and TDP, respectively (Table 1). Irrespective of the sampling periods, the lake samples (L1 to L4) presented lower levels of the organic matter and the nutrient concentrations than those of the upstream catchments (U1 to U4 and I1 to I5) (t test, $p<0.05$). The exceptions were BOD and TDP concentrations in September. The relatively low concentrations in the lake may be attributed to the dilution effect driven by the exchange of the lake water with the nearby seawater. It has been reported that the exchanged water reaches 16 million tons per day, accounting for 8.9 % of the storage capacity of the lake (Cho 2005). Except for BOD, the estuary area showed the concentration ranges of the water quality parameters falling between those of the upstream catchments and the lake (Table 1).

Seasonal variations in the general water quality parameters were compared for each categorized sampling region. The organic pollution of the upstream catchments, which were represented by BOD, COD, and DOC concentrations in average, was more serious in May than in September ($p<0.05$), and the same trend was observed for the nutrient concentrations (i.e., TDP and TN). In the premonsoon season, the pollutants from the industrial and municipal effluents were the least diluted by precipitation. In contrast, the dilution effect could be more pronounced in September, in which much higher precipitation (232 mm) was reported (www.wamis.go.kr) than in May (9 mm). The lower salinity values of the upstream catchments in September versus May (t test, $p<0.05$) also supported the enhanced dilution effect in the monsoon season. However, the lake samples exhibited the opposite trend for the seasonal variations. For example, except for DOC, all the measured parameters of the lake displayed higher concentration levels in September versus May (t test, $p<0.05$) (Table 1). This observation may be explained by the increased pollutant loadings into the lake for the rainy season.

Our results based on the selected water quality parameters demonstrated that the major pollutant sources of the lake stemmed from the upper streams and the industrial channels (i.e., the upstream catchments). It was also notable that the water quality of the lake might be strongly affected by the dilution from the seawater exchange, and it varied seasonally probably due to the catchment runoff. Previous studies on metal and organic contamination of this lake have also shown that the deterioration of the lake water quality originated from anthropogenic activities occurring in the upper catchments (Ra et al. 2011; Moon et al. 2012).

Table 1 Concentrations (mean ± standard deviation) of selected water quality parameters for the four different sampling regions at two different sampling periods[a]

Parameter	Catchments				Estuary		Lake	
	Industrial channels		Upper streams					
	May ($n=5$)	September ($n=5$)	May ($n=4$)	September ($n=4$)	May ($n=2$)	September ($n=2$)	May ($n=8$)	September ($n=8$)
Salinity	0.7 ± 0.2	0.4 ± 0.1	0.3 ± 0.1	0.1 ± 0.0	13.7 ± 10.9	0.7 ± 0.7	28.7 ± 0.2	26.9 ± 1.9
BOD	5.9 ± 1.0	2.9 ± 1.9	4.2 ± 4.0	0.7 ± 0.6	1.1 ± 0.1	1.1 ± 0.4	1.4 ± 0.4	2.2 ± 0.7
COD	72.6 ± 14.2	30.6 ± 12.0	27.5 ± 5.8	16.2 ± 6.0	22.3 ± 6.5	22.8 ± 5.5	5.2 ± 1.0	8.2 ± 2.6
DOC	23.9 ± 14.0	6.3 ± 3.1	6.1 ± 1.7	3.5 ± 1.2	5.6 ± 2.4	4.0 ± 0.2	1.8 ± 0.3	1.9 ± 0.2
TN	4.4 ± 1.7	3.7 ± 0.8	4.7 ± 1.4	2.8 ± 1.4	4.6 ± 4.3	2.9 ± 0.3	0.5 ± 0.0	0.8 ± 0.2
TDP	0.177 ± 0.128	0.100 ± 0.066	0.175 ± 0.155	0.139 ± 0.065	0.170 ± 0.129	0.183 ± 0.025	0.023 ± 0.006	0.070 ± 0.027
Chl a	0.029 ± 0.049	0.002 ± 0.002	0.035 ± 0.038	0.007 ± 0.006	0.028 ± 0.007	0.006 ± 0.004	0.008 ± 0.004	0.002 ± 0.001

[a] The unit of salinity is practical salinity units (psu). The other parameters are in mg L^{-1}

BOD biochemical oxygen demand, *COD* chemical oxygen demand, *DOC* dissolved organic carbon, *TN* total nitrogen, *TDP* total dissolved phosphorus, *Chl a* chlorophyll *a*

Spectroscopic properties of DOM

SUVA has been used as a measure of DOM aromaticity in water samples (Weishaar et al. 2003). For this study, the average SUVA values exhibited large spatial and seasonal variations, ranging from 0.7 to 2.9 L mg C^{-1} m^{-1} (Table 2). However, no seasonal difference was found for the lake. Instead, the samples from the upper streams showed lower SUVA values in September than in May (t test, $p < 0.05$), and the estuary had the same trend. The results suggest that more nonaromatic DOM components could be brought into the estuary presumably from the upstream forested and agricultural areas in the rainy season. No distinct seasonal difference was found for the industrial channels.

Significant positive relationships between CDOM absorption and DOC concentrations were previously reported in aquatic environments, and the CDOM absorption coefficient at 375 nm (i.e., a375) has often been used as a surrogate for colored DOM (Fichot and Benner 2012; Asmala et al. 2012). In this study, the average a375 values of the lake were 1.1 and 0.7 m^{-1} in May and September, respectively (Table 2), which fell within the ranges reported from Danish estuaries and coastal water (Stedmon et al. 2000) and from the open sea (Kowalczuk et al. 2005). The average a375 values of the catchment areas and the estuary had much higher levels,

ranging from 6.7 to 9.5 m^{-1}, indicating that the external DOM sources may contain a larger fraction of chromophoric organic matter within the total pool of DOM compared to the lake DOM. Photobleaching may be involved in lowering a375 values in the lake (Stedmon et al. 2000).

The spectral slope of S$_{275-295}$ ranged from 13.8 to 22.9 µm^{-1} (Table 2), which fell into the range reported from three Finnish estuaries (Asmala et al. 2012). The spectral slopes of the lake were higher than those of the upstream catchments for both sampling periods (t test, $p < 0.05$), which was consistent with the previous studies reporting the higher spectral slope values of water samples with increasing salinity (Helms et al. 2008; Asmala et al. 2012; Fichot and Benner 2012). Based on an inverse relationship previously established between the spectral slope and the molecular weight of DOM (Helms et al. 2008), our result suggests that the molecular size of the lake DOM may be smaller than those of the upstream areas probably due to photobleaching.

The spectral slope ratio (i.e., S$_R$ or S$_{275-295}$/S$_{350-400}$) can be utilized as an indicator of photobleaching (Helms et al. 2008). For this study, the slope ratios presented the range between 1.0 and 2.4 (Table 2). Seasonal differences were observed for all the four classified regions of the lake, and the catchment areas with higher values shown in May versus September (t test, $p < 0.05$) and the estuary had the same trend. This result could

Table 2 Spectroscopic properties (mean ± standard deviation) of DOM for the four different sampling regions at two different sampling periods

Parameters	Upstream Catchments				Estuary		Lake	
	Industrial channels		Upper streams					
	May (n=5)	September (n=5)	May (n=4)	September (n=4)	May (n=2)	September (n=2)	May (n=8)	September (n=8)
SUVA[a]	1.0 ± 0.7	0.7 ± 0.4	2.9 ± 0.5	1.1 ± 0.0	1.9 ± 0.9	1.1 ± 0.2	1.3 ± 0.2	1.3 ± 0.4
S$_{275-295}$[b]	17.8 ± 1.9	16.0 ± 3.1	13.8 ± 1.9	14.4 ± 0.7	15.2 ± 3.5	13.8 ± 0.2	20.2 ± 2.7	22.9 ± 3.1
S$_R$[c]	1.7 ± 0.4	1.3 ± 0.3	1.4 ± 0.1	1.0 ± 0.1	1.4 ± 0.0	1.0 ± 0.1	2.4 ± 0.4	1.1 ± 0.2
a$_{375}$[d]	7.8 ± 3.0	7.6 ± 1.2	9.5 ± 0.6	7.4 ± 3.2	6.7 ± 6.8	8.3 ± 1.3	1.1 ± 0.7	0.7 ± 0.5
FI[e]	1.7 ± 0.0	1.8 ± 0.0	1.7 ± 0.0	1.7 ± 0.1	1.6 ± 0.0	1.6 ± 0.1	1.6 ± 0.0	1.6 ± 0.0
HIX[f]	3.5 ± 1.5	3.6 ± 2.3	6.8 ± 0.6	8.1 ± 0.4	5.2 ± 1.6	6.7 ± 1.4	2.0 ± 0.3	3.2 ± 0.4
A[g]	164.0 ± 51.7	28.1 ± 13.5	72.0 ± 12.6	26.3 ± 6.3	91.9 ± 32.1	14.0 ± 2.0	7.6 ± 1.1	14.7 ± 8.6
C[g]	74.9 ± 33.3	10.1 ± 5.0	43.2 ± 6.9	15.5 ± 4.0	49.2 ± 15.5	7.1 ± 1.6	3.7 ± 0.6	7.3 ± 4.3
T[g]	71.1 ± 78.8	25.8 ± 47.4	14.0 ± 3.5	3.5 ± 0.9	23.3 ± 12.7	2.0 ± 0.1	3.9 ± 0.6	4.2 ± 2.1
M[g]	83.1 ± 28.9	12.3 ± 7.6	40.0 ± 6.8	13.8 ± 3.9	49.4 ± 17.1	6.8 ± 0.9	4.2 ± 0.6	7.6 ± 4.4

[a] Specific UV absorbance in L mg C^{-1} m^{-1} (Weishaar et al. 2003)

[b] Spectral slope in µm^{-1} (Helms et al. 2008)

[c] Spectral slope ratio (Helms et al. 2008)

[d] Absorbance coefficient at 375 nm in m^{-1} (Stedmon et al. 2000)

[e] Fluorescence index (McKnight et al. 2001)

[f] Humification index (Zsolnay et al. 1999)

[g] Fluorescence intensities of humic-like peak A, humic-like peak C, tryptophan-like peak T, and marine humic-like peak M (Coble 2007) in quinine sulphate units (QSU)

Fig. 2 EEM plots of DOM samples in May (*left side*) and in September (*right side*). **a**, **b** Surface samples from L2 site in the lake. **c**, **d** Samples from E1 site in the estuary. **e**, **f** Samples from I4 site in the industrial channels. **g**, **h** Samples from U1 site in the upper streams
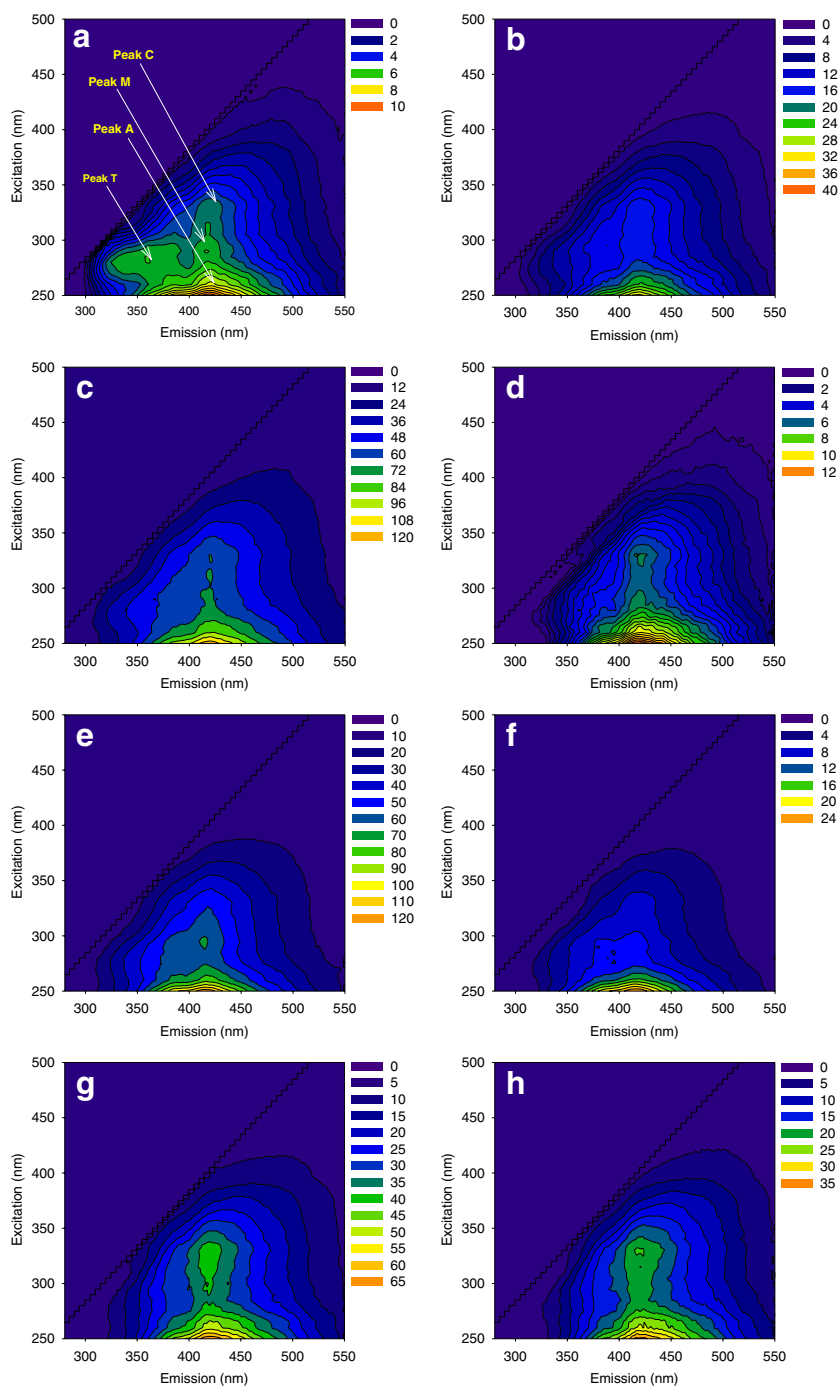
be attributed to the seasonal difference in the local solar radiation. Longer monthly sunshine hours were reported for this study area in May (525–540 h per month) compared to September (420–435 h per month) (http://www.greenmap.go.kr). The observed seasonal differences in the spectral slope ratios were much pronounced for the lake (i.e., 128.4 % difference) than for the upstream catchments (41.6 % difference) and the estuary (43.1 % difference), presumably due to longer

residence time and photobleaching effects on DOM (i.e., lower molecular weight) (Helms et al. 2008).

For this study, all the samples showed similar FI values ranging from 1.6 to 1.8. However, the average HIX values of the upstream catchments exhibited higher levels compared to those of the lake, and higher HIX values were observed for the lake in September than in May (*t* test, $p < 0.05$). The HIX information implies that, for the rainy season, more humified

and condensed DOM structures from the upstream catchments may be accumulated in the lake, subsequently affecting the composition of the lake DOM.

Fluorescence EEM

Four peaks were identified from the EEM plots of all the samples (Fig. 2). The peak maxima were located at the excitation/emission wavelengths of <250/410–430 nm, 310–330/410–430 nm, 280–300/410–430 nm, and 270–280/330–360 nm. Following the definitions of Coble (2007), they can be categorized as humic-like peak A, humic-like peak C, marine humic-like peak M, and tryptophan-like peak T, respectively. Seasonal differences were found in the EEM peaks. Except for the lake, all the peak maxima were higher in May than in September (Table 2). The differences were even more pronounced compared to those of the DOC concentrations (Table 1), suggesting that seasonal variability may be much greater for fluorescent DOM compounds compared to the total pool of DOC. Peak M was also observed for the samples from the catchments, not only from the lake, implying that the marine humic-like fluorescence features could be present for the areas where biological activity is much involved (i.e., anthropogenic and/or agricultural sources (Hudson et al. 2007).

EEM-PARAFAC components

Three fluorescence components (C1, C2, and C3) were decomposed from the EEM measurements for all 38 samples from the two seasons by the PARAFAC modeling (Fig. 3). The overlap of the excitation and the emission loadings of the two halves on the whole dataset confirmed that the three components were appropriate to represent the measured fluorescence EEM dataset (Stedmon et al. 2003). No outliers were found. C1 exhibited a primary (and secondary) fluorescence maximum intensity at an excitation/emission wavelength of <250 (280)/382 nm. This component was analogous to the peak M in the previous EEM plots, which was reportedly associated with the primary production of phytoplankton in oceans and freshwaters (Coble 2007). Similar PARAFAC components were reported for other DOM samples, and they were assigned as microbial humic-like components in prior studies (Stedmon et al. 2003; Yamashita et al. 2011). The appearance of the peak may also be attributed to the production of new CDOM due to microbial degradation of labile organic substitutes (Hur et al. 2009; Zhang et al. 2011). From incubation experiments using axenic cultures of phytoplankton, for example, (Romera-Castillo et al. 2010) reported that the microbial humic-like components were possibly generated by the biotransformation of algal-derived organic matters. For our study, however, no significant correlation was observed between Chl a and the PARAFAC component. Instead, the highest correlation was found between C1 and DOC

concentrations ($r=0.793$, $p<0.0001$) among the three PARAFAC components, suggesting that anthropogenic organic matter may be largely involved for the presence of the component. Similarly, Zhang et al. (2011) claimed that this component was highly associated with the anthropogenic factors such as land use and human activities of the upstream catchments for the downstream Tianmuhu lake, China.

C2 presented a fluorescence peak at the excitation/emission wavelengths of 280/320 nm, which resembles Peak T in the EEM plots (Coble 2007). This component is commonly observed for many aquatic samples that are subject to anthropogenic influences in bays, estuaries, coastal areas, as well as the areas of high primary productivity (Stedmon and Markager 2005; Yamashita et al. 2008; Hong et al. 2012). Although many studies implied substantial contribution of phytoplankton to the component of coastal and lake waters (Hanamachi et al. 2008; Zhang et al. 2009), there is still lack of the correlation between Chl a and the component (i.e., C2) (Yamashita et al. 2011). This study also showed no direct relationship between Chl a and C2 ($r=0.076$; $p=0.651$). Instead, there was a close association between C1 and C2 ($r=0.978$, $p<0.0001$), suggesting that the two fluorophore groups may be similar to each other in their organic sources.

C3 exhibited a primary and a secondary fluorescence maxima at the excitation/emission wavelengths of <250/425 nm and 330/425 nm, respectively. The component appears to be the mixture of the two humic-like fluorescence peaks previously observed (i.e., peak A and peak C). Prior studies demonstrated that the component 3 might be either terrestrially derived or possibly produced autochthonously in aquatic environments largely affected by terrestrial input (Stedmon and Markager 2005; Guo et al. 2011; Zhang et al. 2011; Murphy et al. 2008).

The relative distributions of the three PARAFAC components, expressed by the percent component, were compared for all the sampling regions at the two different sampling periods in Fig. 4. Irrespective of the sampling seasons, the highest abundance of C1 over all the three components (i.e., %C1) was observed for the industrial channels, suggesting that the component may be closely related to the anthropogenic organic pollution. Meanwhile, %C3 was the highest among the three components for the upper streams and the estuary, implying a close association between C3 and terrestrial carbon sources (Fig. 4). Except for the industrial channels, C3 appears to be more pronounced for all the samples in September than in May, also suggesting that terrestrial organic input from the forested and agricultural catchments into the lake may be intensified during the rainy season.

PCA for the interpretation of spatial and seasonal variations in DOM

The basic matrix in PCA was constructed based on 15 different variables of each sample (Fig. 5). The sampling site of I1

Fig. 3 PARAFAC model output showing the three fluorescent components (*left*) and the corresponding excitation/ emission loadings (*right*). Excitation/emission loadings consist of two independent halves of the dataset (*red* and *blue dotted lines*) and the complete dataset (*black lines*)
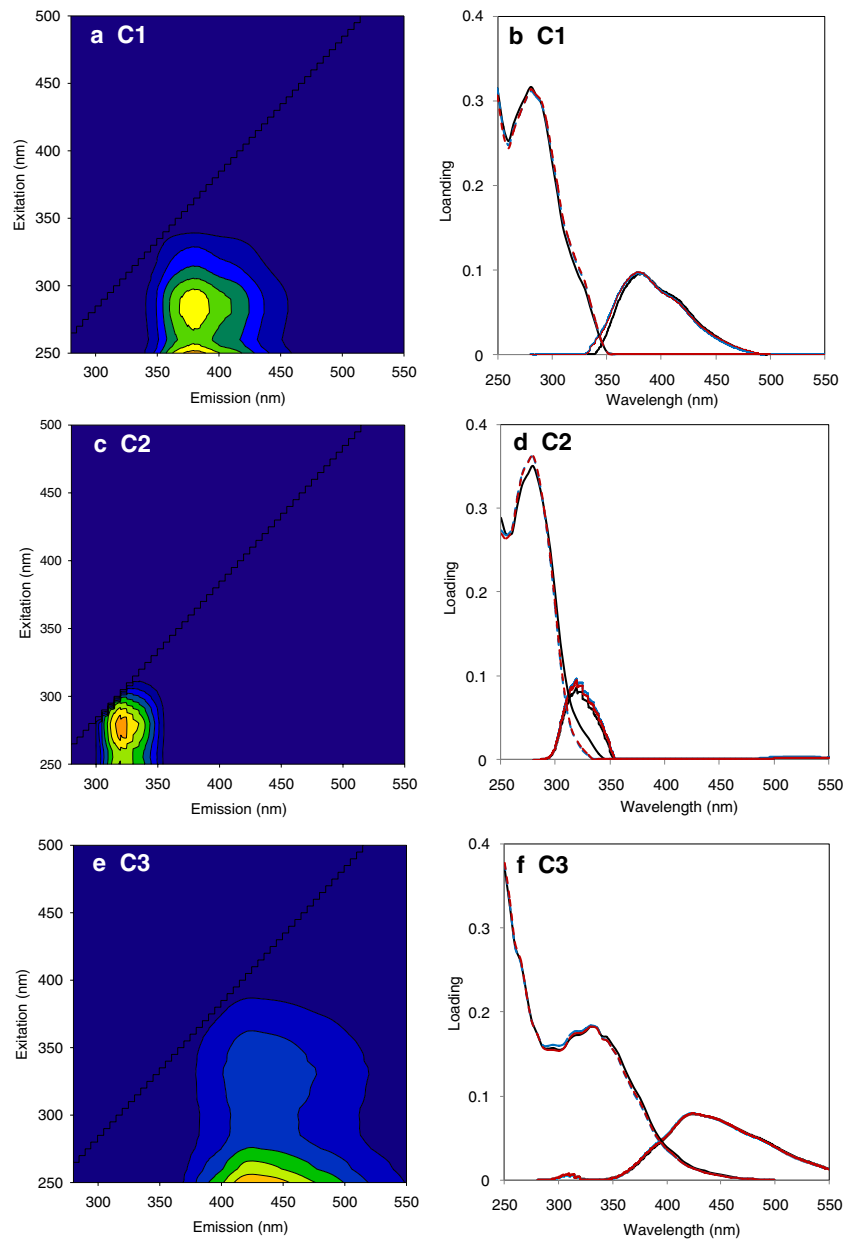

Fig. 4 Relative distributions (%) of the three PARAFAC components for the four different sampling regions in **a** May and **b** September
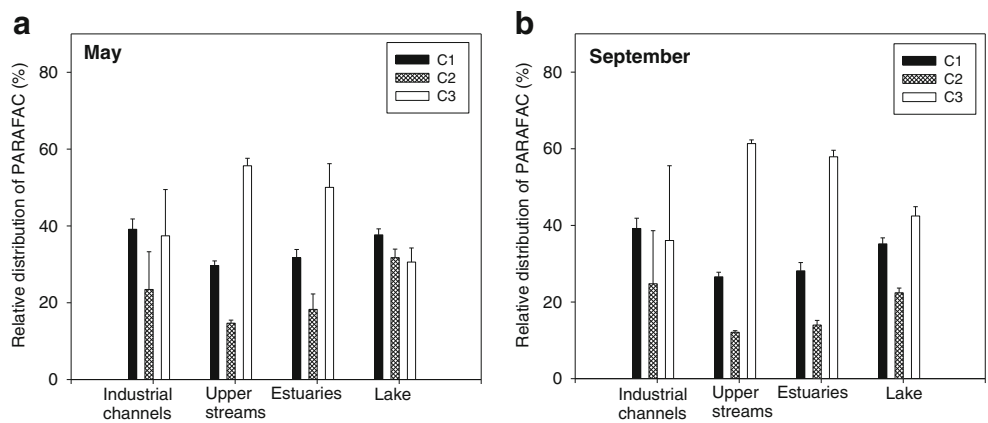
Fig. 5 Principal component analysis of selected water quality parameters and spectroscopic properties of DOM for all the samples with the exception of I1 site (see the text). **a** Loading plot. **b** Score plot. The *hollow* and *solid* symbols represent the samples collected in May and September, respectively. Note that Shapiro-Wilk test confirmed normality in the distribution of each parameter included in the PCA ($p < 0.05$)
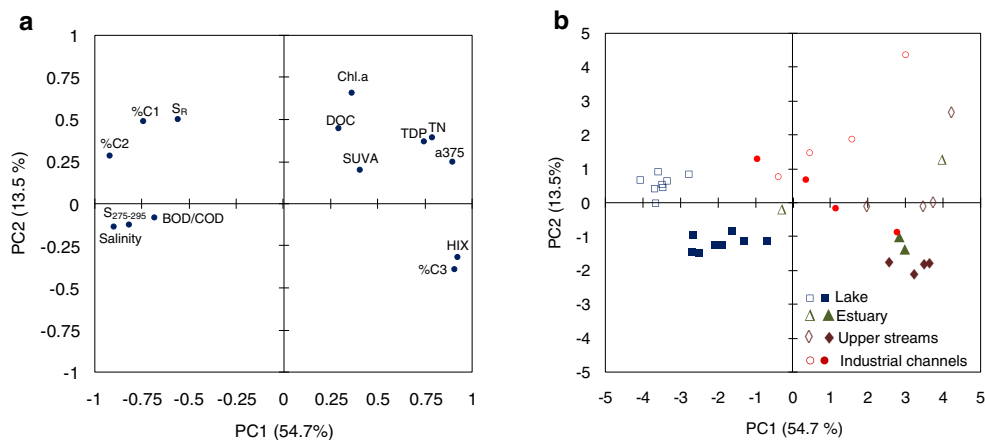
was excluded from the PCA because of a concern that the extremely high concentrations of the general water quality parameters may yield bias in the interpretation of the results. For this study, the first two principal components explained over 69.9 % of the total data variance. Correlations between the first two principal components and the measured properties were depicted in a loading plot (Fig. 5a). The first principal component (PC1) was responsible for the 50.3 % variance. Positive high loadings on PC1 were observed for the variables of salinity, %C2, and $S_{275-295}$, whereas the high negative loadings were observed for a375, HIX, %C3, and nutrients. PC2 represents 19.7 % of the total variability, and it has positive loading with organic-matter-related water quality parameters and %C1 and negative loadings with %C3 and HIX (Fig. 5a). From the overall locations of the variables in the loading plot, it can be postulated that PC1 is an indicator to discriminate between marine organic matter and anthropogenic and/or terrestrial organic matter originating from the upstream catchments, whereas PC2 is related to the concentrations of DOM. The location of %C2 close to salinity suggests that the presence of C2 may be associated with autochthonous production in marine environments.

Additional information on seasonal differences was obtained from the score plot (Fig. 5b). The lake DOM showed the unique characteristics distinguished from either the industrial channels or the upper streams, as demonstrated by the distinctive location of the lake samples from the two catchment sources. Furthermore, the lake samples could be easily separated into two seasons in the plot, as the September samples were located toward the left side of the PC1 axis than those of May. This observation suggests that, in September, the lake DOM is likely to be more affected by terrestrial input from the upstream catchments. Such seasonal differences were observed for other sampling regions, as the data points corresponding to the monsoon season were located in the lower positions along the PC2 axis, indicating that more condensed organic carbon components of allochthonous origin may be more dominant for the rainy season irrespective of the

sampling sites. Our PCA results provided additional evidence that the dilution effects from the seawater exchange may govern the characteristics of DOM and the water quality in the lake. The variability of the lake DOM appears to be partially affected by seasons as well, exhibiting higher contribution of the organic input from the upper catchments to the lake for the monsoon versus the premonsoon seasons.

Conclusions

Although the upstream catchments were the major sources of DOM and nutrients to the coastal lake, much lower concentration levels were observed in the lake due to the dilution effect from the seawater exchange. The CDOM properties of the lake were distinguished from those dissolved organic matter sources from the upstream catchments. Lower absorption coefficients, HIX values, fluorescence EEM peak intensities, and higher spectral slopes were obtained from the lake samples, in comparison to values of the upper catchments, suggesting that the lake DOM is characterized by lower molecular size and less condensed structures. Seasonal differences were also found for the upper streams and the lake, in which higher absorption coefficients and fluorescence peak intensities but lower spectral slopes and HIX values were exhibited for the premonsoon versus the monsoon season. In contrast, the seasonal differences were much less pronounced for the industrial channels except for fluorescence peaks. PARAFAC modeling revealed that a combination of three fluorophore groups explained the variations in the fluorescence features of the DOM samples. The high abundance of C1 component (microbial humic-like) in the samples from the industrial channels suggests that this component may be associated with anthropogenic organic pollution. C3 component (terrestrial humic-like) was the most enriched for the samples from the upper streams and the estuary, and the relative distribution was greater for the rainy season. Our PCA results based on spectroscopic properties of DOM revealed that

although the lake DOM was the most likely to be affected by the dilution effect, the contribution of allochthonous DOM input from the upstream catchments to the lake might be elevated during the rainy season.

References

APHA (American Public Health Association), AWWA (American Water Works Association), & WEF (Water Environment Federation) (2005) Standard methods for the examination of water and waste-water (20th ed.). Washington DC, USA

Asmala E, Stedmon CA, Thomas DN (2012) Linking CDOM spectral absorption to dissolved organic carbon concentrations and loadings in boreal estuaries. Estuar Coast Shelf Sci 111: 107–117

Chari N, Sarma NS, Pandi SR, Murthy KN (2012) Seasonal and spatial constraints of fluorophores in the midwestern Bay of Bengal by PARAFAC analysis of excitation emission matrix spectra. Estuar Coast Shelf Sci 100:162–171

Cho DO (2005) Lessons learned from Lake Shiwha Project. Coast Manag 33(3):315–334

Cho YS, Lee JW, Jeong W (2012) The construction of a tidal power plant at Sihwa Lake, Korea. Energ Source Part A 34(14):1280–1287

Coble PG (2007) Marine optical biogeochemistry: the chemistry of ocean color. Chem Rev 107(2):402–418

Coble PG, Del Castillo CE, Avril B (1998) Distribution and optical properties of CDOM in the Arabian Sea during the 1995 Southwest Monsoon. Deep-Sea Res PT II 45(10–11):2195–2223

Fichot CG, Benner R (2012) The spectral slope coefficient of chromophoric dissolved organic matter (S275-295) as a tracer of terrigenous dissolved organic carbon in river-influenced ocean margins. Limnol Oceanogr 57(5):1453–1466

Fuentes M, Gonzalez-Gaitano G, Garcia-Mina JM (2006) The usefulness of UV-visible and fluorescence spectroscopies to study the chemical nature of humic substances from soils and composts. Org Geochem 37(12):1949–1959

Guo WD, Yang LY, Hong HS, Stedmon CA, Wang FL, Xu J, Xie YY (2011) Assessing the dynamics of chromophoric dissolved organic matter in a subtropical estuary using parallel factor analysis. Mar Chem 124(1–4):125–133

Hanamachi Y, Hama T, Yanai T (2008) Decomposition process of organic matter derived from freshwater phytoplankton. Limnology 9(1):57–69

Helms JR, Stubbins A, Ritchie JD, Minor EC, Kieber DJ, Mopper K (2008) Absorption spectral slopes and slope ratios as indicators of molecular weight, source, and photobleaching of chromophoric dissolved organic matter. Limnol Oceanogr 53(3):955–969

Hong HS, Yang LY, Guo WD, Wang FL, Yu XX (2012) Characterization of dissolved organic matter under contrasting hydrologic regimes in a subtropical watershed using PARAFAC model. Biogeochemistry 109(1–3):163–174

Hudson N, Baker A, Reynolds D (2007) Fluorescence analysis of dissolved organic matter in natural, waste and polluted waters—a review. River Res Appl 23(6):631–649

Hur J, Jung NC, Shin JK (2007) Spectroscopic distribution of dissolved organic matter in a dam reservoir impacted by turbid storm runoff. Environ Monit Assess 133(1–3):53–67

Hur J, Park MH, Schlautman MA (2009) Microbial transformation of dissolved leaf litter organic matter and its effects on selected organic matter operational descriptors. Environ Sci Technol 43(7):2315–2321

KICOX (Korea Industrial Complex Corporation) (2011) Industrial park development in Korea economy: a guideline for development and management of industrial parks. Seoul, Korea, 152 pp

KORDI (Korea Ocean Reasearch and Development Institute) (1999) A study on environmental changes of Shihwa lake by outer seawater inflow (3rd year). KORDI Report, Asan, Korea, 363 pp

Kowalczuk P, Ston-Egiert J, Cooper WJ, Whitehead RF, Durako MJ (2005) Characterization of chromophoric dissolved organic matter (CDOM) in the Baltic Sea by excitation emission matrix fluorescence spectroscopy. Mar Chem 96(3–4):273–292

Kowalczuk P, Durako MJ, Young H, Kahn AE, Cooper WJ, Gonsior M (2009) Characterization of dissolved organic matter fluorescence in the South Atlantic Bight with use of PARAFAC model: Interannual variability. Mar Chem 113(3–4):182–196

Maie N, Yamashita Y, Cory RM, Boyer JN, Jaffe R (2012) Application of excitation emission matrix fluorescence monitoring in the assessment of spatial and seasonal drivers of dissolved organic matter composition: Sources and physical disturbance controls. Appl Geochem 27(4):917–929

McKnight DM, Boyer EW, Westerhoff PK, Doran PT, Kulbe T, Andersen DT (2001) Spectrofluorometric characterization of dissolved organic matter for indication of precursor organic material and aromaticity. Limnol Oceanogr 46(1):38–48

Moon HB, Choi M, Yu J, Jung RH, Choi HG (2012) Contamination and potential sources of polybrominated diphenyl ethers (PBDEs) in water and sediment from the artificial Lake Shihwa, Korea. Chemosphere 88(7):837–843

Mulholland PJ (2003) Large-scale patterns in dissolved organic carbon concentration, flux, and sources. In: Findlay S, Sinsabaugh RL (eds) Aquatic ecosystems Interactivity of dissolved organic matter. Aquatic Ecology Series. Academic Press, San Diego, pp 139–160

Murphy KR, Stedmon CA, Waite TD, Ruiz GM (2008) Distinguishing between terrestrial and autochthonous organic matter sources in marine environments using fluorescence spectroscopy. Mar Chem 108(1–2):40–58

Nguyen HVM, Lee MH, Hur J, Schlautman MA (2013) Variations in spectroscopic characteristics and disinfection byproduct formation potentials of dissolved organic matter for two contrasting storm events. J Hydrol 481:132–142

Ra K, Bang JH, Lee JM, Kim KT, Kim ES (2011) The extent and historical trend of metal pollution recorded in core sediments from the artificial Lake Shihwa, Korea. Mar Pollut Bull 62(8):1814–1821

Romera-Castillo C, Sarmento H, Alvarez-Salgado XA, Gasol JM, Marrase C (2010) Production of chromophoric dissolved organic matter by marine phytoplankton. Limnol Oceanogr 55(1):446–454

Romera-Castillo C, Nieto-Cid M, Castro CG, Marrase C, Largier J, Barton ED, Alvarez-Salgado XA (2011) Fluorescence: absorption coefficient ratio—tracing photochemical and microbial degradation processes affecting coloured dissolved organic matter in a coastal system. Mar Chem 125(1–4):26–38

Stedmon CA, Markager S (2005) Resolving the variability in dissolved organic matter fluorescence in a temperate estuary and its catchment using PARAFAC analysis. Limnol Oceanogr 50(2):686–697

Stedmon CA, Markager S, Kaas H (2000) Optical properties and signatures of chromophoric dissolved organic matter (CDOM) in Danish coastal waters. Estuar Coast Shelf Sci 51(2):267–278

Stedmon CA, Markager S, Bro R (2003) Tracing dissolved organic matter in aquatic environments using a new approach to fluorescence spectroscopy. Mar Chem 82(3–4):239–254

Thurman EM (1985) Organic geochemistry of natural waters. Martinus Nijhoff/Dr W. Junk Publishers, Dordrecht, The Netherlands, 497 pp

Weishaar JL, Aiken GR, Bergamaschi BA, Fram MS, Fujii R, Mopper K (2003) Evaluation of specific ultraviolet absorbance as an indicator of the chemical composition and reactivity of dissolved organic carbon. Environ Sci Technol 37(20):4702–4708

Won EJ, Hong S, Ra K, Kim KT, Shin KH (2012) Evaluation of the potential impact of polluted sediments using Manila clam *Ruditapes philippinarum*: bioaccumulation and biomarker responses. Environ Sci Pollut Res 19(7):2570–2580

Yamashita Y, Jaffe R, Maie N, Tanoue E (2008) Assessing the dynamics of dissolved organic matter (DOM) in coastal environments by excitation emission matrix fluorescence and parallel factor analysis (EEM-PARAFAC). Limnol Oceanogr 53(5):190–1908

Yamashita Y, Cory RM, Nishioka J, Kuma K, Tanoue E, Jaffe R (2010) Fluorescence characteristics of dissolved organic matter in the deep waters of the Okhotsk Sea and the northwestern North Pacific Ocean. Deep-Sea Res Part II-Top Stud Oceanogr 57(16):1478–1485

Yamashita Y, Panton A, Mahaffey C, Jaffe R (2011) Assessing the spatial and temporal variability of dissolved organic matter in Liverpool Bay using excitation-emission matrix fluorescence and parallel factor analysis. Ocean Dyn 61(5):569–579

Yoo H, Yamashita N, Taniyasu S, Lee KT, Jones PD, Newsted JL, Khim JS, Giesy JP (2009) Perfluoroalkyl Acids in marine organisms from Lake Shihwa, Korea. Arch Environ Contam Toxicol 57(3):552–560

Zhang YL, van Dijk MA, Liu ML, Zhu GW, Qin BQ (2009) The contribution of phytoplankton degradation to chromophoric dissolved organic matter (CDOM) in eutrophic shallow lakes: field and experimental evidence. Water Res 43(18):4685–4697

Zhang YL, Yin Y, Feng LQ, Zhu GW, Shi ZQ, Liu XH, Zhang YZ (2011) Characterizing chromophoric dissolved organic matter in Lake Tianmuhu and its catchment basin using excitation-emission matrix fluorescence and parallel factor analysis. Water Res 45(16):5110–5122

Zsolnay A, Baigar E, Jimenez M, Steinweg B, Saccomandi F (1999) Differentiating with fluorescence spectroscopy the sources of dissolved organic matter in soils subjected to drying. Chemosphere 38(1):45–50